Two dimensional boron nitride growth on nickel foils by plasma assisted molecular beam epitaxy from elemental B and N sources

Walter Batista-Pessoa, Xavier Wallart, Dominique Vignaud

Two dimensional boron nitride growth on nickel foils by plasma assisted molecular beam epitaxy from elemental B and N sources

Walter Batista-Pessoa, Xavier Wallart, Dominique Vignaud*

Université de Lille, CNRS, Centrale Lille, JUNIA ISEN, Université Polytechnique Hauts de France, UMR 8520-IEMN F-59000 Lille France

*Corresponding author: dominique.vignaud@univ-lille.fr

Abstract

The growth of two dimensional sp^2-bonded boron nitride (2D-BN) was studied in a plasma-assisted molecular beam epitaxy set-up, using independent boron and nitrogen sources. We studied the growth conditions on polycrystalline Ni foils: B and N respective fluxes, growth temperature and time, which are influencing the surface morphology, stoichiometry and the 2D-BN domain size. Using a B/N precursor flux ratio >>1 yields films with incorporated boron largely in excess and intermixed with 2D-BN. On the contrary, precursor flux ratios from moderately B-rich to moderately N-rich leads to stoichiometric 2D-BN. The optimum growth temperature is found to be 900°C, a temperature for which the crystallographic quality is improved compared to lower temperatures thanks to the increased adatom surface mobility although a partial sublimation of BN occurs. Increasing the growth time under the optimized settings shows that the growth does not occur in a layer-by-layer mode, but rather by stacking BN domains on top of each other with a rather slow lateral extension of the domains.

1. Introduction

Hexagonal boron nitride (hBN) is a two-dimensional Van der Waals insulator with a wide bandgap (~6 eV). It is chemically and thermally stable making it exceptionally interesting as an ultrathin barrier, tunneling or passivation layer for integrated electronics and photonics [1]. It is also an ideal candidate for graphene encapsulation, preserving the properties of high quality graphene for future devices. It must be remembered that hexagonal boron nitride is one of many two dimensional boron nitride polytypes (2D-BN) [2], including all sp^2-bonded boron nitrides with different stacking such as the stable phases AAô (hexagonal) or ABC (rhombohedral) [3]. The graphene-like AB stacking was rarely observed, involving different structures such as stacking faults in rhombohedral BN [4] or as metastable inclusions in hBN bulk crystals [5].

Although hBN is a promising material for many breakthrough applications, no technique is yet able to grow defect free hBN in large surface. The main top-down approach, mechanical exfoliation, is limited to surfaces of a few 100 µm² at most. On the contrary, bottom-up techniques (such as chemical vapor deposition (CVD), molecular beam epitaxy (MBE), pulsed laser deposition, etc.) should be scalable but still face significant challenges to grow high quality hBN at the wafer scale [6]. For bottom-up techniques to be able to produce continuous hBN films with well-controlled thickness, thorough studies of the interaction between the precursors and substrate are mandatory. In the case of MBE, using a boron effusion cell and a nitrogen plasma source facilitates this task because only two elements are used, compared to CVD that needs precursors and carrier gases making their interactions more complex. Using elemental B and N cells offers the possibility to adjust independently the B and N fluxes that reach the substrate, but also to study individually the impact of each element during growth and their respective interactions with the substrate. Growing 2D-BN on Ni is highly dependent on the Ni grain orientation. The calculated surface energy is the highest for (100) grains, then for (110), and significantly decreases for (111) orientation [7]. By using the ammonia-borane precursor in a low pressure CVD reactor, it was observed that the 2D-BN growth was faster on (001) grains while 2D-BN could not be detected on (111) grains [8]. The morphology of the grown 2D-BN depends on the Ni grain orientation, changing from a ñcotton flowerò shape on Ni(001) to a flatter parallel morphology resulting from the epitaxial relationship between the BN and the Ni(111) surface [4]. The interaction between hBN and nickel also plays an essential role on the growth. The first 2D-BN layer grown on nickel is chemisorbed due to the strong hybridization between the Ni 3d and hBN-´ states [9].

Under ultra-high vacuum (UHV) environment, borazine or a combination of a high-temperature boron effusion cell with a remote radio-frequency (RF) N-plasma source were the most studied set of precursors to grow 2D-BN. Ammonia was seldom used as an alternative nitrogen source, without requiring a plasma cell, associated to B_2H_6 gas [10] or to B_2O_3 powder [11]. The 2D-BN thickness is

self-limited to one monolayer on Ni with the borazine precursor, because the catalyzed fragmentation of borazine by Ni stops when the 2D-BN coverage is complete [12, 13]. On the other hand, using a boron effusion cell and a remote N-plasma cell allows to overcome such thickness limitation to obtain multilayers 2D-BN [14-16]. This technique might be referred to as plasma-assisted MBE (PAMBE). The hBN morphology was observed to change from dendritic, star-shaped islands to triangular domains when increasing the temperature from 730 to 835°C [15]. Growth temperatures from 700°C [16] to 890°C [14] were reported. The published transmission electron microscopy images and reflected high energy electron diffraction patterns suggest that a high quality multilayer hBN epitaxially grown on Ni(111) was elaborated, despite using a rather low temperature of 700°C [16]. It is not yet clear how such a good result could be obtained at the lowest reported growth temperature, it may result from the initial Ni buffer layer grown onto the monocrystalline substrate. Other preliminary Ni treatments such as carburization or electropolishing were also able to improve hBN growth. It was claimed that the hBN 2D growth mode was favored by tuning the carbon interstitial concentration [11]. It was also observed that electropolishing leads to a higher BN growth rate, resulting from the increased density of nucleation sites [17].

With PAMBE, while the growth temperature can be straightforwardly studied, the same is not true for the B/N precursor flux ratio which appears more complex to understand due to the variety of the nitrogen active species produced by the plasma cell and of their interactions with the substrate. In this work, we investigated the growth conditions to obtain 2D-BN on polycrystalline Ni foils. We studied the impact of the B atomic flux, growth temperature, N plasma-cell settings and growth time. A thorough analysis of how each growth parameter influences the 2D-BN stoichiometry, morphology and thickness is presented and optimal growth conditions are obtained.

2. Experiments

2D-BN films were grown by PAMBE in a commercial RIBER UHV chamber, using an infrared pyrometer at 0.85 µm wavelength for growth temperature measurements. More details about this chamber were already published [13, 18]. We used a high-temperature effusion cell for the boron source (MBE-Komponenten), with high purity (5N) elemental boron granules loaded in a graphite crucible. The nitrogen cell is a radio-frequency valve plasma cell (VRF-N-600 from RIBER) designed to optimize the amount of atomic species while minimizing the emitted ionic species. The maximum RF power and N_2 flow are respectively 600 W and 10 sccm. The plasma optical intensity is measured by an optical sensor (signal in volts) in the range 750-850 nm, corresponding to the atomic nitrogen spectral range [19]. 25µm thick polycrystalline nickel foils purchased from Alfa-Aesar were used as substrate (specified purity 99.99%). They were cleaned in acetone and isopropanol and finally deoxidized in acetic acid just before loading in the UHV chamber. The Ni foils were first annealed at

950°C in the MBE chamber for at least 2 hours for removal of any residual organic matter and oxides. It results in grains of typical size between 5 and 100 µm, without any preferential orientation. The BN growth step took place just after this pre-annealing. Table 1 summarizes the experimental parameter range of our experiments. We first explored the impact of the boron atomic flux by varying the B-cell temperature from 1700°C to 1850°C. Then, we studied the growth temperature from 800°C to 960°C. Finally, we optimized the impact of the nitrogen plasma cell by varying the N_2 flow and power as well as the growth time up to 240 min.

boron cell temperature (°C)	1700, 1760, 1800, 1850
nitrogen plasma cell settings, RF power (W) / N_2 flow (sccm) / plasma optical signal (V)	a) 480/5/2.5, b) 540/1.5/2.5 or c) 580/5/3.1
growth temperature (°C)	800, 900, 930, 960
N_2 growth pressure (Torr) / N_2 flow (sccm)	$6\ 10^{-6}$ / 1.5 or $2.5\ 10^{-5}$ / 5
growth time (min)	60, 120, 240

Table 1. Experimental parameter ranges investigated for the growth of 2D-BN on Ni.

Samples were transferred under air exposure to the X-ray photoelectron spectroscopy (XPS) chamber for chemical analysis as well as BN thickness estimation. The measurements were realized using a Physical Electronics 5600 spectrometer fitted in an UHV chamber (base pressure $\sim 1 \cdot 10^{-10}$ Torr). Spectra were recorded using a monochromatized Al anode X-ray source (photon energy 1487 eV), a pass energy of 12 eV and a typical probe size of 400 µm diameter. The B/N composition ratio was determined from the I_{B1s}/I_{N1s} integrated intensity ratio, corrected for the instrument relative sensitivity as calibrated after a measurement on exfoliated hBN [18]. I_{B1s} (respectively I_{N1s}) represents the total integrated intensity of the BN-related B1s (N1s) component, and I_{Ni2p} stands for the integrated intensity of the Ni2p3/2 substrate peak. The ratios I_{B1s}/I_{Ni2p} and I_{N1s}/I_{Ni2p} obtained for different photoelectron angles were used to estimate the averaged BN thickness based on a homogeneous thickness single layer model [13]. The detection angle corresponds to the angle between the surface and the direction of the photoelectrons and was varied between 25° (close to grazing incidence, surface sensitive) and 75° (nearly normal incidence, bulk sensitive). All the spectra presented here were obtained for a 45° angle. The surface morphology was analyzed with a Zeiss Supra 55 scanning electron microscope (SEM) using an InLens detector, i.e. by measuring backscattered electrons along the beam direction. The incident electron beam was set to 1 keV for better surface sensitivity. In the case of 2D-BN, the InLens intensity increases with the 2D-BN thickness [20]. Raman spectra were measured using a Horiba Scientific LabRAM HR confocal spectrometer with a 473 nm laser spot (power ~10mW). The beam was focused to a size smaller than 1 µm by a 100x objective.

3. Results and discussion

When growing 2D-BN by PAMBE, the flux of injected species reaching the sample surface plays a key role on the film stoichiometry, thickness as well as morphology. The impact of the atomic boron flux was firstly analyzed by varying the B-cell temperature T_B from 1700 to 1850°C, resulting in an estimated B flux ratio of 11 [21] between the highest and lowest flux (see table 2). The N_2 plasma cell conditions were kept constant (1.5 sccm N_2 flow with 540 W RF power), as well as the substrate temperature (800°C) and the duration (1 h). Typical B1s and N1s spectra are shown in figure 1, while examples of their spectral deconvolutions are presented in the insets (for T_B=1760°C). Two components related to B-N bonds are observed in both spectra, as well as a third one related to B-Ni or B-B bonds in the B1s 187-189 eV range. Because of the strong hybridization between the Ni 3d and the 2D-BN π states of the first 2D-BN layer, one observes a binding energy difference of ~1 eV between the metallic coupled 2D-BN layer at the interface and the uncoupled components for films thicker than one monolayer, consistent with the already reported values [9]. So, the experimental curve fitting was achieved using an asymmetric component for the lowest binding energy peak (corresponding to the 1st layer with a metallic behavior resulting from the coupled bonds) [9, 13], and a symmetric component at higher binding energy for the uncoupled insulating ones (see inserts of figure 1, where the coupled component is plotted in red and the uncoupled one in blue). The B/N composition ratios reported here were calculated from the total integrated intensity ratio I_{B1s}/I_{N1s} for the sum of both BN-related components (see table 2).

B cell temperature (°C)	relative B flux	XPS B/N ratio	excess boron (%)	2D-BN thickness (monolayer)	incident B/N flux ratio
1700	1	1.02	3.2	2.9	< 1
1760	2.5	1.02	3.7	4.2	~1
1800	5.0	1.03	4.7	4.4	> 1
1850	11	1.05	51	< 8	>> 1

Table 2. The relative B flux, as evaluated from the temperature-dependent pressure of boron [21], as a function of the B-cell temperature. The B/N composition ratio, as determined from the corresponding XPS integrated intensity ratio corrected for set-up sensitivity, for 2D-BN grown on Ni under constant activated N flux. The B/N composition ratio was determined considering the sum of the coupled and uncoupled BN-related XPS components. The percentage of boron in excess is evaluated from the integrated intensity of the B1s peak with maxima in the 187-189 eV binding energy range divided by the total integrated intensity of B1s. The 2D-BN thickness was evaluated from the B1s/Ni2p and N1s/Ni2p integrated intensity ratio. The indicative incident flux ratio conditions were deduced from the analysis of the XPS measurements.

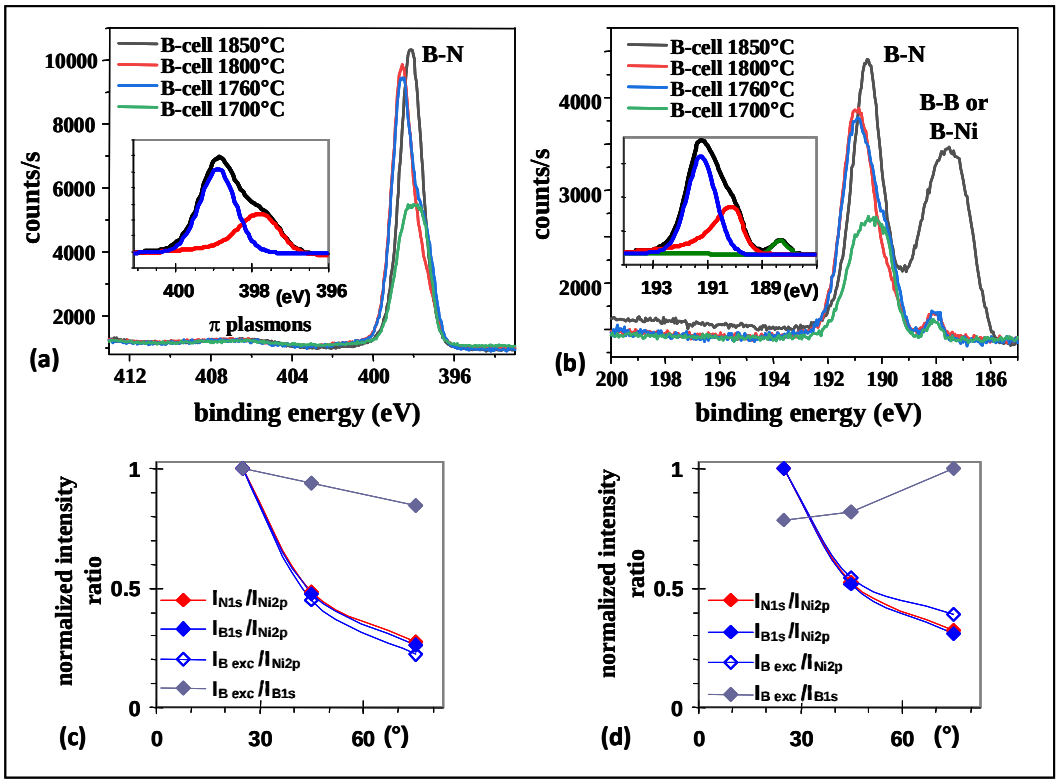

Figure 1: XPS measurements of 2D-BN samples grown at 800°C during 1 hour under fixed nitrogen plasma-cell settings (1.5 sccm, 540 W), while varying the atomic B flux by adjusting the B-cell temperature T_B from 1700 to 1850°C, (a) N1s region showing the overlapping uncoupled and coupled components, respectively located at ~398 eV and ~397 eV, (b) B1s region also showing the overlapping uncoupled and coupled components at ~191 eV and ~190 eV , as well as an extra well-separated B1s peak related to B-B and/or B-Ni bonds. Inserts in panels a and b correspond to the deconvolution of the 2D-BN spectra for a sample grown with the B-cell set at 1760°C. Angle-resolved XPS experiments, normalized intensity ratios are plotted for growth at T_B= 1850°C (c) and 1800°C (d) vs the photoelectron emission angle, where the 25° (respectively 75°) angle is close to grazing (normal) incidence.

According to the literature, the extra B1s component in the 187-189 eV range may be related either to B-Ni [22, 23] or B-B bonds [22, 24, 25]. Both are located almost at the same binding energy due to their very close electronegativity (2.04 eV for B and 1.91eV for Ni [26]). Nonetheless, we can reasonably assume that the B1s extra component is mostly related to B-B bonds for the highest B flux (at T_B=1850°C), in which case it is located at 187.5 eV. Indeed, reducing the B flux (T_B=1800°C) results in a strong decrease of this extra peak intensity and in a slight shift towards a higher binding energy at 188.2 eV. With a further reduction of the B flux down to the lowest value explored in this study, the peak position remains nearly constant while its intensity slowly decreases, representing ~3% of the B1s total surface for the lowest B flux (at T_B=1700°C, see table 2). We expect it to be the

amount of the B atoms which are located at the interface or have diffused into the Ni matrix (~0.3 at% solubility of B in Ni at 1085°C [27]), to form compounds such as $Ni_{23}B_6$ [28]. These assignments to B-B bonds for the highest B flux, and to B-Ni for a reduced B flux (with a B-cell temperature set in the range 1700-1800°C) are qualitatively consistent with the angular-dependency of the intensity ratios which are displayed in figures 1c (for T_B=1850°C) and 1d (T_B=1800°C). The normalized intensity ratio I_{Bexc}/I_{B1s} shows a very different angular behavior in these two cases (where I_{Bexc} is the total integrated intensity of the bonds involving excess boron atoms, that is the non BN-related B1s component with a maximum in the 187-189 eV range, see figure 1b). For the highest B flux, this ratio is the largest at low angles (figure 1c) which means that the corresponding B-B bonds are close to the surface. On the contrary, when the B flux is reduced, the maximum I_{Bexc}/I_{B1s} ratio is obtained at close to normal angles (figure 1d), so that the related bonds are located deeper in the sample than the 2D-BN, probably at the BN/Ni interface or into the Ni ôbulkô, and thus involve B-Ni bonds.

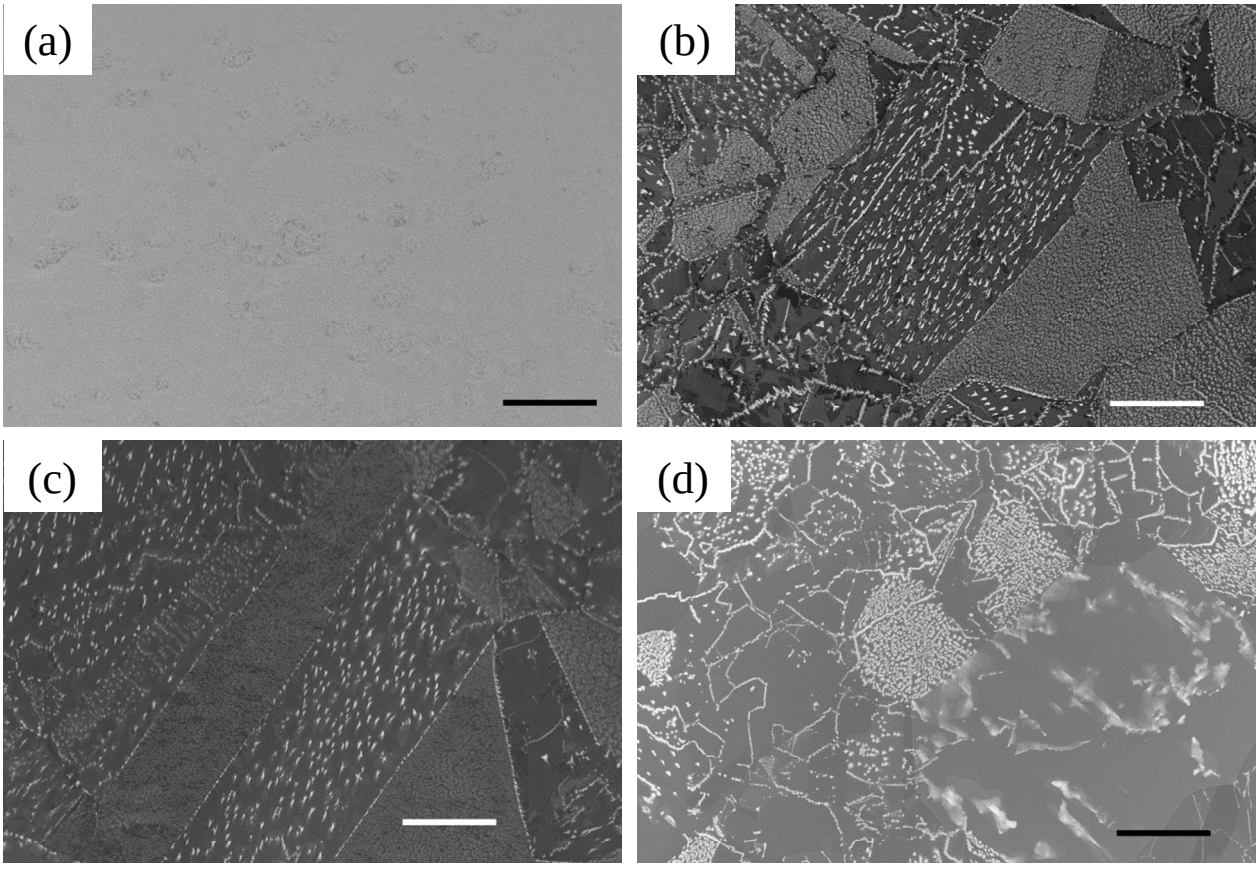

Figure 2: SEM images of samples grown at 800°C during 1 hour under fixed nitrogen plasma conditions (1.5 sccm N_2, 540 W), while varying the atomic B flux by setting the B-cell temperature at 1850°C (a), 1800°C (b), 1760°C (c) or 1700°C (d) (scale bars 50 µm). The 2D-BN morphology depends on the Ni grain orientation, it ranges from granulous BN to tiny BN triangular domains (up to ~7 µm long).

The B flux has a significant impact on the 2D-BN structure as well as on its thickness, as evaluated from the XPS intensity ratios I_{B1s}/I_{Ni2p} and I_{N1s}/I_{Ni2p}. This is illustrated in the SEM images displayed in figure 2. The corresponding 2D-BN average thicknesses are indicated in table 2. Under ultra-rich boron environment (T_B=1850°C), the incident B/N precursor flux ratio is much larger than 1. Almost 50% of the B1s XPS total intensity comes from non-nitrogen bonded B atoms, the excess boron (see table 2). We were unable to identify 2D-BN domains by SEM, but only an almost structure-free surface resulting of an intermixing between excess boron and BN (see figure 2a). Indeed, the angular-dependent variations of the XPS integrated intensities shown in figure 1d show that the distribution of excess B and 2D-BN are almost identical. In this case, the BN thickness deduced from the I_{B1s}/I_{Ni2p} and I_{N1s}/I_{Ni2p} ratios is strongly overestimated because the excess boron also contributes to the Ni substrate intensity attenuation, resulting in an overestimation of these ratios and thus of the total BN thickness.

When the B flux is reduced (T_B=1760 or 1800°C), the amount of excess B is reduced to 4-5% of the total boron atoms. 2D-BN domains are observed on the surface with a maximum length of ~7µm. The corresponding surface morphologies are similar (see figures 2b and 2c) as well as the estimated BN thickness of ~4 monolayers, despite a ~2 times increase of the B flux (for T_B=1800°C compared to the T_B=1760°C case, see table 2). For a B-cell temperature set at 1800°C, we assume that the excess incident B atoms are not incorporated in the growing film since no significant difference on the BN thickness and on the excess boron percentage could be deduced from the XPS measurements. This suggests that the T_B=1800°C condition corresponds to a B-rich precursor flux, and that the BN growth rate is limited by the incoming active nitrogen species which are all incorporated in the 2D-BN layer. With a further reduction of the B flux (T_B=1700°C), the 2D-BN average thickness decreases compared to the previously discussed cases. This is consistent with the B flux being now the limiting factor for 2D-BN growth. The overall conditions are then nitrogen-rich (incident precursor flux ratio B/N < 1) and all B atoms reaching the surface participate to the 2D-BN growth. SEM observations show that the amount of granulous 2D-BN is reduced (see figure 2d). Since growth with a B-cell set at 1700°C (1800°C respectively) corresponds to N-rich (B-rich) incident precursor fluxes, the intermediate case with the B-cell at 1760°C is probably the one closest to the B/N ~1 stoichiometric precursor flux conditions (which are gathered in the last column of table 2). We have chosen to study next the growth of 2D-BN under a moderately B-rich environment (T_B=1800°C), to avoid the incorporation of excess B obtained with higher fluxes while preserving the possibility to increase the plasma cell active N flux for material optimization.

Besides the B/N flux ratio, another critical parameter is the growth temperature, which may affect the BN stoichiometry, the BN thickness as well as the film morphology. From the analysis of the XPS spectra, the higher temperature to grow 2D-BN on Ni is 900°C, above which the B and N sticking coefficients are significantly reduced and their incorporation is no longer balanced. In this last case, a

very thin non-stoichiometric BN sub-coverage layer is only grown (for which B/N > 1.5, see table 3). At 800°C and 900°C, stoichiometric BN films are obtained. The 2D-BN layer estimated thickness is reduced at 900°C compared to 800°C (see figure 3 and table 3), suggesting that a limited sublimation

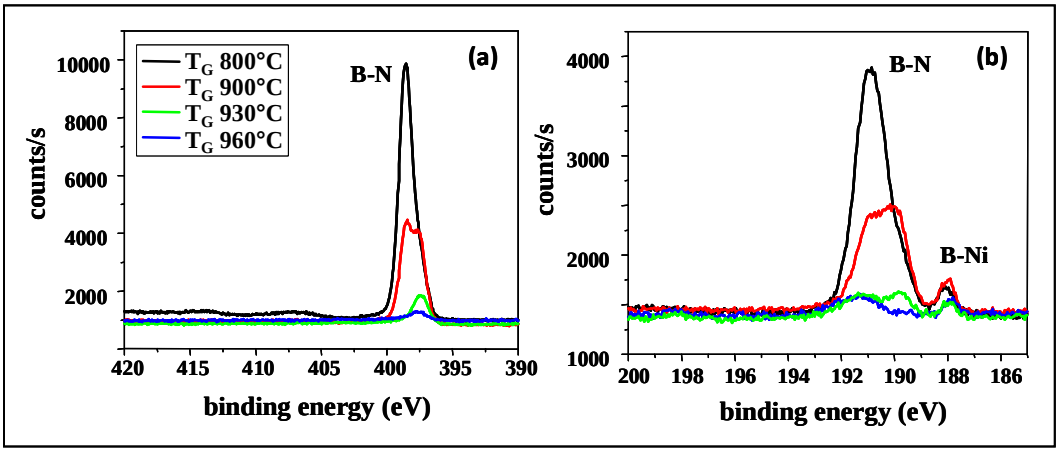

Figure 3: XPS measurements of 2D-BN samples grown with the B-cell temperature set at 1800°C and the nitrogen plasma cell at 1.5 sccm N2 and 540 W RF power for one hour, as a function of the growth temperature TG, N1s range (a) and B1s range (b).

of adsorbed B and N atoms is already occurring at 900°C, although it does not affect the stoichiometry of the 2D-BN. Despite the reduced estimated thickness obtained at the highest usable growth temperature of 900°C, the corresponding increase of the B and N adatom surface mobility is expected to result in an improvement of the 2D-BN domain crystallography. Growing 2D-BN at 800°C not only yields granular material in many Ni grains but also tiny obtuse triangular islands with a long side up to 7 µm (see figure 2c). Increasing the temperature to 900°C results in smoother 2D-BN and most importantly to well defined triangular islands with maximum side length of ~10µm (see figures 4a and 4b). These observations of the evolution of the 2D-BN domain shape towards more regular triangles while increasing the growth temperature are consistent with the results already presented [15]. Figure 4c shows the Raman measurements recorded at several spots on the sample surface (indicated by colored arrows in figure 4b). The triangular domain 2D-BN peak intensity at ~1370 cm^{-1} clearly increases with the 2D-BN thickness while the peak full width at half-maximum decreases down to 14 cm^{-1}. It is important to point out that the measurements carried out in the dark regions in the SEM figure 4b do not show any 2D-BN Raman signature. For the darkest zones, which correspond to single layer areas, this results from the coupling between the first BN layer and the Ni substrate, which makes the BN metallic [9, 11]. For few layer 2D-BN, the Raman peaks were not detected either, most probably because the 2D-BN thickness is very low, as already discussed [29, 18]. Therefore, the optimum growth temperature for 2D-BN on Ni is 900°C and has been used for all samples described in the followings.

growth temperature (°C)	XPS B/N ratio	2D-BN thickness (monolayer)
800	1.03	4.4
900	1.01	2.8
930 or 960	> 1.5	no BN

Table 3. The B/N composition ratio and the 2D-BN average thickness determined from the XPS analysis of the intensity ratios I_{B1s}/I_{N1s} , I_{B1s}/I_{Ni2p} and I_{N1s}/I_{Ni2p} as a function of the growth temperature.

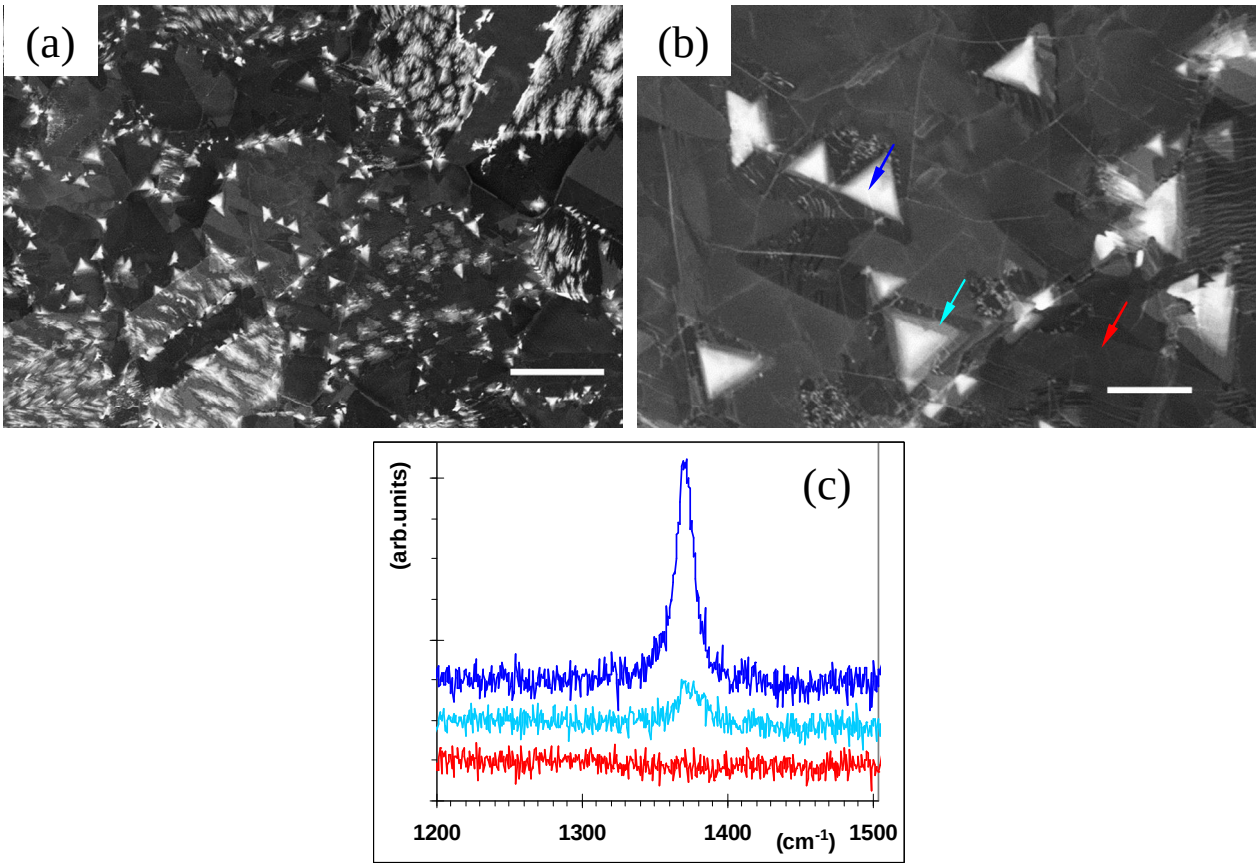

Figure 4: (a) SEM image of a 2D-BN sample grown at 900°C during 1 hour under fixed nitrogen plasma conditions (1.5 sccm N2, 540 W) and B-cell temperature (1800°C) (scale bar 50 µm), (b) zoom (scale bar 10 µm) in the central area of panel (a), where arrows point to the areas where the Raman spectra shown in (c) were measured. No BN Raman signal (red curve in panel c) could be detected in the darker areas shown in (b) (see red arrow in the lower right corner).

The influence of the nitrogen plasma cell settings (N_2 flux and RF power) was studied under a moderately B-rich growth environment (T_B=1800°C), so that variations on the flux of the nitrogen

active species could be directly observed. We studied three plasma-cell settings (see table 1). Settings a (1.5 sccm N_2 and 540 W) and b (5 sccm N_2 and 480 W) result in identical plasma optical intensities (~2.5 V) from a very different combination of N_2 flux and RF power, while settings c (5 sccm N_2 and 580 W) was selected to obtain the highest plasma optical intensity (~3.1 V) allowed by the set-up. From the analysis of the XPS measurements shown in figure 5 and of the corresponding intensity ratios I_{B1s}/I_{N1s}, the 2D-BN composition is found to be stoichiometric for the three plasma-cell settings. In the case of the two samples grown with the same optical plasma intensity (settings a and b), one observes a limited change on the relative intensities of the coupled and uncoupled components (figures 5a and 5b), and the average thickness estimated from the XPS integrated intensities are identical (see figure 5c). For settings c for which the plasma emission is the most intense, an average ~40% thicker

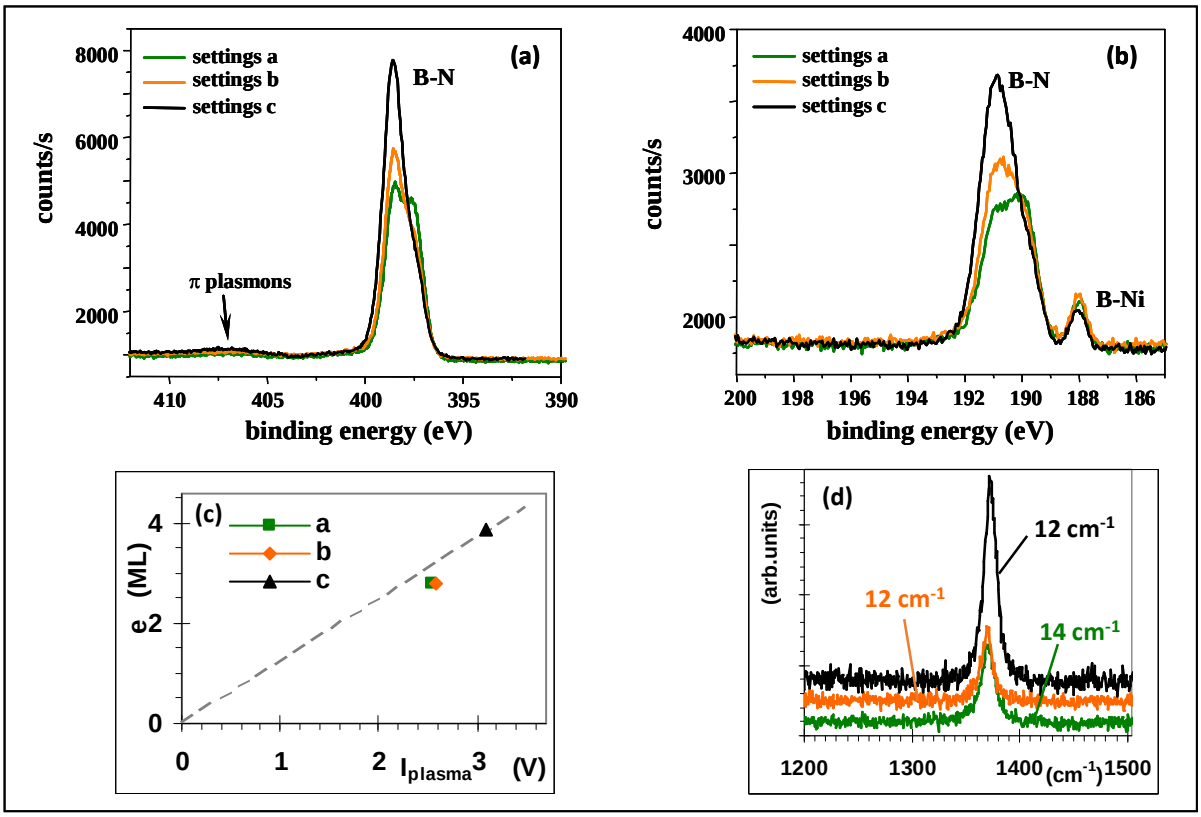

Figure 5: 2D-BN films grown for one hour at 900°C with the B-cell set at 1800°C using different plasma-cell settings, a (1.5 sccm N2 flow, 540 W RF power, green curve), b (5 sccm, 480 W, orange curve) or c (5 sccm, 580 W, black curve), corresponding XPS spectra in the N1s (a) and B1s (b) ranges. All three conditions yield stoichiometric 2D-BN. Panel (c) displays the 2D-BN average thickness vs the optical plasma intensity for all three plasma-cell settings for one hour growth (the dashed line is just a linear guide). Typical Raman spectra measured on the thickest triangular domains for one hour grown samples are shown in panel (d), with indication of the Lorentzian fit full-

width at half-maximum (spectra are vertically shifted for clarity). The same color code is used in all panels for identifying the plasma-cell settings.

2D-BN layer is obtained, if compared to the thickness for the a and b settings (figure 5c). This directly comes from the active N flux increase for settings c. The 2D-BN estimated thickness is approximatively proportional to the optical plasma intensity (see figure 5c), although the limited range explored does not allow for a definitive conclusion at this time. This linear correlation suggests that the precursor fragments active for the growth of 2D-BN are the monoatomic nitrogen atoms responsible for the light emission in the wavelength range measured by the detector. A similar behavior was already mentioned in a study of the growth of GaN films using a similar optical plasma intensity detector [30]. Typical Raman spectra were recorded at the triangular domains which appear with a white contrast in SEM pictures (see figure 4b and 6d), corresponding to the thickest 2D-BN domains. They are shown in figure 5d for the three plasma-cell settings. A slightly wider peak was measured for settings a. Also, a significantly more intense peak was observed with settings c, which could be partially explained by the relative thickness increase compared to the other settings a and b. This set of observations shows that the plasma-cell settings c lead to the best quality material. Therefore, we now focus our attention on samples grown using these settings.

SEM images in figure 6 show how the 2D-BN morphology evolves with the growth time using the optimized growth parameters found in the previous experiments. With our set-up, this corresponds to a growth temperature of 900°C, a boron cell temperature of 1800°C and a plasma-cell working at 580 W RF power with a 5 sccm N_2 flow, We observe on the low magnification images (figures 6a to 6c) that the BN domains get more densely packed with growth time, although the coverage is not yet homogenous after 4 hours. The 2D-BN triangular domains are easily found at higher magnification (figures 6d to 6f), showing their horizontal as well as stacking structure. This set of images shows that the maximum 2D-BN domain size increases from ~12 µm (1 h, figure 6d) up to ~24 µm (4 h, figure 6f). Lateral growth of the 2D-BN is still effective after 4 hours, although it is slowing down. It must be also mentioned that a complete homogeneous coverage is not obtained when the different domains start to coalesce. A similar structure involving triangular domains was already reported for growth of 2D-BN on identical polycrystalline Ni foils but from a different set of precursors, gaseous borazine and activated nitrogen [18]. The current observations confirm the role of the Ni grain orientation on the 2D-BN structure previously discussed [18].

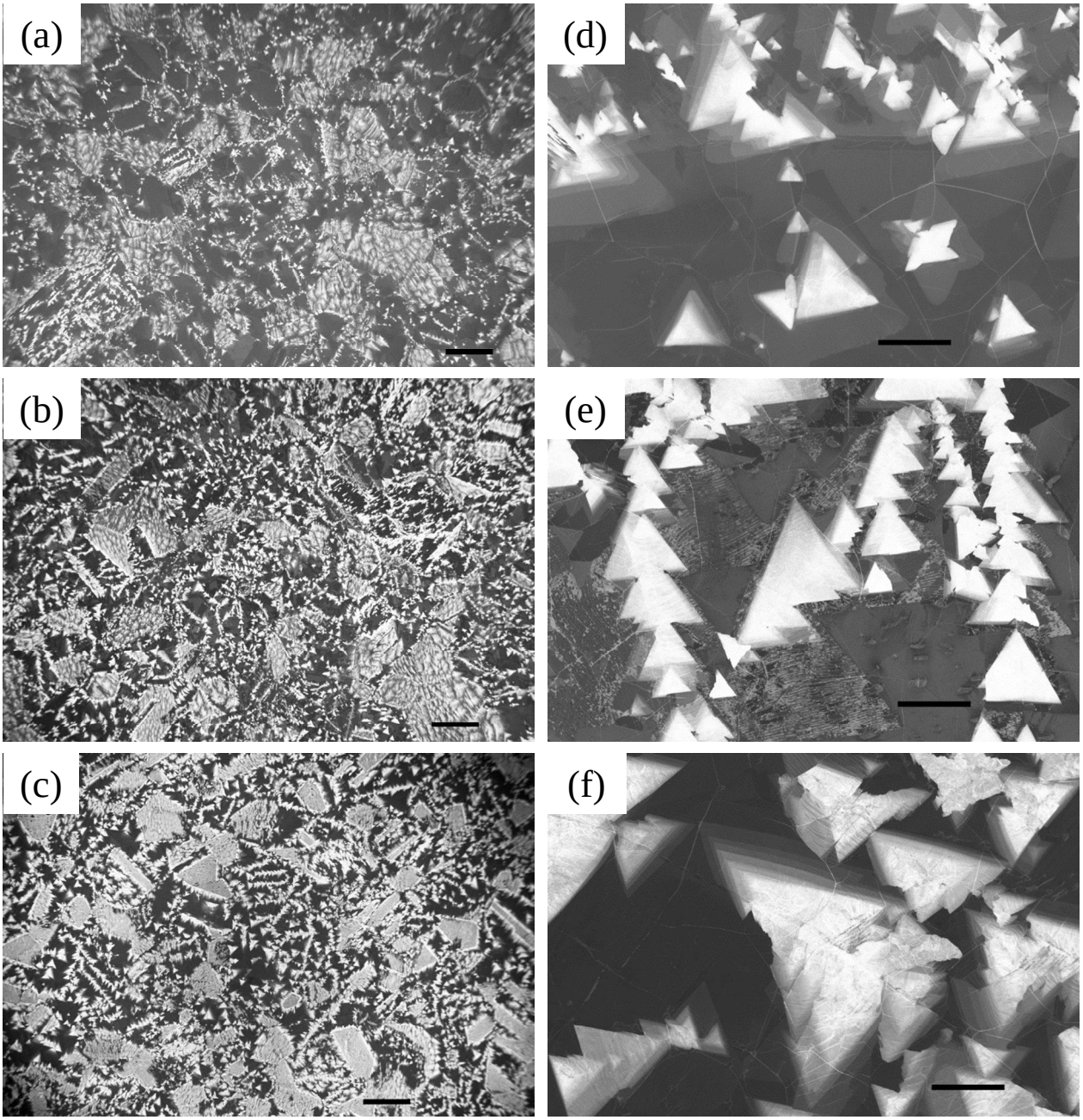

Figure 6: 2D-BN optimized growth at 900°C with B-cell set at 1800°C and N-plasma power and N2 flux set at 580 W and 5.0 sccm respectively, as a function of the growth time of 1 h (a,d), 2 h (b, e) and 4 h (c, f). SEM images with 100x magnification show the overall film morphology on polycristalline Ni consisting of triangular domains and granulous areas (a,b,c, scale bars 100 µm)). Zoom with a higher magnification (1540x) show the 2D-BN triangular domains being stacked onto each other (d, e, f, scale bars 10 µm).

4. Conclusions

We performed a thorough study on the growth conditions of 2D-BN on Ni foils using boron and nitrogen elemental sources in a plasma-assisted MBE set-up. The strong hybridization between 2D-BN and nickel, already observed when using the gaseous precursor borazine, also occurs in this case, as shown by XPS measurements. The binding energy difference between 2D-BN coupled and uncoupled components is around 1 eV. The B/N precursor flux ratio plays a fundamental role on the 2D-BN properties. It can be tuned by adjusting the B cell temperature as well as the N-plasma cell settings (RF power and N_2 flow). Under highly B-rich conditions, boron in excess is incorporated in the growing film, intermixed with BN which is not stoichiometric. When using almost well-balanced B and N flux, from slightly B-rich to slightly N-rich, 2D-BN is grown with a limited amount of residual boron bonded with Ni, either located at the interface or diffused into the Ni matrix. The N precursor flux depends on two independent physical parameters, the RF power and the N_2 flow. Our results suggest that the optical plasma intensity measured in the monoatomic nitrogen spectral emission range is a well-suited parameter to quantify the average growth rate, regardless of the N_2 flux and RF power combination. Using our optimized growth conditions, regular 2D-BN triangular domains are obtained, showing typical sizes up to 24 µm. The 2D-BN growth takes place mainly by stacking BN domains on top of each other with a limited lateral extension of the domains. This clearly does not correspond to a layer by layer growth mode, and leads to a rather heterogeneous 2D-BN film on Ni.

Acknowledgments: The financial supports by the 2DHetero FLAG-ERA 2019 project and the French RENATECH network are greatly acknowledged.

References

[1] A. Pakdel, Y. Bando and D. Golberg, *Nano boron nitride flatland*, Chem. Soc. Rev. 43, 934 (2014).

[2] B. Gil, W. Desrat, A. Rousseau, C. Elias, P. Valvin, M. Moret, J. Li, E. Janzen, J.H. Edgar, G. Cassabois, *Polytypes of sp²-bonded boron nitride*, Crystals 12, 782 (2022).

[3] K. Watanabe and T. Taniguchi, *Hexagonal boron nitride as a new ultraviolet luminescent materials and its application*, Int. J. Appl. Ceram. Technol. 8, 977 (2011)

[4] H. Prevost, A. Andrieux-Ledier, N. Dorval, F. Fossard, J.S. Mérot, L. Schué, A. Plaud, E. Héripré, J. Barjon and A. Loiseau, *Heteroepitaxial growth of sp²-hybridized bor on nitride multilayer on nickel substrates by CVD: the key role of the substrate orientation*, 2D Mater. 7, 045018 (2020).

[5] A. Rousseau, P. Valvin, W. Desrat, L. Xue, J. Li, J.H. Edgar, G. Cassabois and B. Gil, *Bernal boron nitride crystals identified by deep-ultraviolet cryomicroscopy*, ACS Nano 16, 2756 (2022)

[6] J.M.J. Lopes, *Synthesis of hexagonal boron nitride: from bulk crystals to atomically thin films*, Prog. Crystal Growth Charac. Mat. 67, 100522 (2021)

[7] L. Vitos, A.V. Ruban, H.L. Skriver, J. Kollár, *The surface energy of metals*, Surf. Sci. 411, 186 (1998).

[8] Y.H. Lee, K.K. Liu, A.Y. Lu, C.Y. Wu, C.T. Lin, W. Zhang, C.Y. Su, C.L. Hsu, T.W. Lin, K.H. Wei, Y. Shi and L.J. Li, *Growth selectivity of hexagonal-boron nitride layers on Ni with various crystal orientations*, RSC Adv. 2, 111 (2012).

[9] A.B. Preobrajenski, A.S. Vinogradov and N. Mårtensson. *Ni 3dï BN ´ hybridization at the hī BN ù Ni(111) interface observed with core-level spectroscopies*, Phys. Rev. B 70, 165404 (2004).

[10] P.C. Mende, Q. Gao, A. Ismach, H. Chou, M. Widom, R. Ruoff, L. Colombo, R.M. Feenstra, *Characterization of hexagonal boron nitride layers on nickel surfaces by low-energy electron microscopy*, Surface Sci. 659, 31 (2017).

[11] H. Tian, A. Khanaki, P. Das, R. Zheng, Z. Cui, Y. He, W. Shi, Z. Xu, R. Lake and J. Liu, *Role of carbon interstitials in transition metal substrates on controllable synthesis of high-quality large-area two-dimensional hexagonal boron nitride layers*, Nano Lett. 18, 3352 (2018).

[12] A. Nagashima, N. Tejima, Y. Gamou, T. Kawai and C. Oshima, *Electronic dispersion relations of monolayer hexagonal boron nitride formed on the Ni(111) surface*, Phys. Rev. B 51, 4606 (1995).

[13] J. Hadid, I. Colambo, C. Boyaval, N. Nuns, P. Dudin, J. Avila, X. Wallart and D. Vignaud, *Molecular beam epitaxial growth of hexagonal boron nitride on Ni foils*, 2D Mater. 8, 045007 (2021).

[14] C.L. Tsai, Y. Kobayashi, T. Akasaka, M. Kasu, *Molecular beam epitaxial growth of hexagonal boron nitride*, J. Crystal Growth 311, 3054 (2009)

[15] S. Nakhaie, J.M. Wofford, T. Schumann, U. Jahn, M. Ramsteiner, M. Hanke, J.M.J. Lopes and H. Riechert, *Synthesis of atomically thin hexagonal boron nitride films on nickel foils by molecular beam epitaxy*, Appl. Phys. Lett. 106, 213108 (2015).

[16] A.A. Tonkikh, E.N. Voloshina, P. Werner, H. Blumtritt, B. Senkovskiy, G. Güntherodt, S.S.P. Parkin and Y.S. Dedkov, *Structural and electronic properties of epitaxial multilayer h-BN on Ni(111) for spintronics applications*, Sci. Rep. 6, 23547 (2016).

[17] Y. He, Y. Li, M. Isarraraz, P. Jena, J. Tran, L. Xu, H. Tian, T. Yang, P. Wei, C.S. Ozkan and J. Liu, *Robust nanocapacitors based on wafer-scale single-crystal hexagonal boron nitride monolayer film*, ACS Appl. Nano Materials 4, 5685 (2021).

[18] J. Hadid, I. Colambo, J. Avila, A. Plaud, C. Boyaval, D. Deresmes, N. Nuns, P. Dudin, A. Loiseau, J. Barjon, X. Wallart and D. Vignaud, *Molecular beam epitaxial growth of multilayer*

2D-boron nitride on Ni substrates from borazine and plasma-activated nitrogen, Nanotechnology 34, 035601 (2023).

[19] H. Carrère, A. Arnoult, A. Ricard, E. Bedel-Pereira. *RF plasma investigations for plasma-assisted MBE growth of (Ga,In)(As,N) materials*, J. Crystal Growth 243, 295 (2002).

[20] P. Sutter and E. Sutter, *Thickness determination of few-layer hexagonal boron nitride films by scanning electron microscopy and Auger electron spectroscopy*, Appl. Phys. Lett. Mater. 2, 092502 (2014).

[21] R.C. Paule and J.L. Margrave, *A Langmuir determination of the sublimation pressure of boron*, J. Phys. Chem. 67, 1368 (1963).

[22] H. Li, H. Li, W.L. Dai, W. Wang, Z. Fang & J.F. Deng, *XPS studies on surface electronic characteristics of Ni B and Ni P amorphous alloy and its correlation to their catalytic properties*, Appl. Surf. Sci. 152, 25 (1999).

[23] F. Muench, M. Oezaslan, M. Rauber, S. Kaserer, A. Fuchs, E. Mankel, J. Brötz, P. Strasser, C. Roth, W. Ensinger, *Electroless synthesis of nanostructured nickel and nickel-boron tubes and their performance as unsupported ethanol electrooxidation catalysts*, J. Power Sources 222, 243 (2013).

[24] P.R. Kidambi, R. Blume, J. Kling, J.B. Wagner, C. Baehtz, R.S. Weatherup, R. Schloegl, B.C. Bayer and S. Hofmann, *In situ observations during chemical vapor deposition of hexagonal boron nitride on polycrystalline copper*, Chem. Mater. 26, 6380 (2014).

[25] B. Feng, J. Zhang, Q. Zhong, W. Li, S. Li, H. Li, P. Cheng, S. Meng, L. Chen & K. Wu, *Experimental realization of two-dimensional boron sheets*, Nature Chem. 8, 563 (2016).

[26] L. Pauling, *The nature of the chemical bond*, 3rd edition, Cornell University Press, Ithaca, N.Y. (1960)

[27] P. Rogl and J.C. Schuster, *Phase diagrams of ternary boron nitride and silicon nitride systems*. ASM International, Ohio (1992).

[28] K.Y. Ma, L. Zhang, S. Jin, Y. Wang, S.I. Yoon, H. Hwang, J. Oh, D.S. Jeong, M. Wang, S. Chatterjee, G. Kim, A.R. Jang, J. Yang, S. Ryu, H.Y. Jeong, R.S. Ruoff, M. Chhowalla and H.S. Shin, *Epitaxial single-crystal hexagonal boron nitride multilayers on Ni (111)*, Nature 606, 88 (2022).

[29] R.V. Gorbatchev, I. Riaz, R.R. Nair, R. Jalil, L. Britnell, B.D. Belle, E.W. Hill, K.S. Novoselov, K. Watanabe, T. Taniguchi, A.K. Geim and P. Blake, *Hunting for monolayer boron nitride: optical and Raman signatures*, Small 7, 465 (2011).

[30] K. Klosek, M. Sobanska, G. Tchutchulashvili, Z.R. Zytkiewicz, H. Teisseyre, L. Klopotowski. *Optimization of nitrogen plasma source parameters by measurements of emitted light intensity for growth of GaN by molecular beam epitaxy*, Thin Solid Films 534, 107 (2013).